Nonlinear Analysis: Modelling and Control, Online First, 1–21
https://doi.org/10.15388/namc.2025.30.38981

Vilnius University Press

Bifurcation analysis of a Leslie–Gower predator–prey system with fear effect and constant-type harvesting*

Chenyang Huangfu, Zhong Li[1]

School of Mathematics and Statistics, Fuzhou University,
Fuzhou, Fujian 350108, China
lizhong04108@163.com

Received: September 30, 2024 / **Revised:** February 5, 2025 / **Published online:** March 3, 2025

Abstract. This paper investigates the effect of fear effect and constant-type harvesting on the dynamic of a Leslie–Gower predator–prey model. Initially, an analysis is carried out to identify all potential equilibria and evaluate their stability. Furthermore, the dynamic behavior at these points is examined, revealing various bifurcations such as saddle-node bifurcation, Hopf bifurcation, and Bogdanov-Takens bifurcation. In particular, the model undergoes a degenerate Hopf bifurcation, which leads to the existence of two limit cycles. Additionally, we demonstrate that the Bogdanov–Takens bifurcation of codimension 2 occurs in this model. Ultimately, these findings are validated through numerical simulations, demonstrating that continuous harvesting or the significant fear effect is not conducive to either predator or prey surviving.

Keywords: predator–prey, fear effect, harvesting, bifurcation.

1 Introduction

The classical Lotka–Volterra predator–prey model was considered by incorporating a logistic growth factor for prey and various population-dependent response functions, and was realised by the mathematical simulation of the interaction between prey and predator. However, the Leslie–Gower predator–prey system [10] is a different model, where the prey population determines the carrying capacity of predator, emphasising that there is an upper limit to the growth rate for both predator and prey. The dynamic behaviour of Leslie–Gower predator–prey system has been extensively researched by many scholars [7, 18–20].

Since the majority of natural resources are renewable, harvesting is a very common practice. In order to study the interaction between two species in a developed ecosystem, several harvesting types have been proposed such as fixed harvesting, fixed effort

*This work was supported by the Natural Science Foundation of Fujian Province (2021J01613).
[1]Corresponding author.

harvesting, continuous threshold harvesting, and nonlinear harvesting. Zhu and Lan [22] considered the following Leslie–Gower predator–prey model incorporating constant-type harvesting in prey:

$$\begin{aligned} \dot{x} &= rx\left(1-\frac{x}{K}\right)-axy-h, \\ \dot{y} &= sy\left(1-\frac{y}{nx}\right), \end{aligned} \tag{1}$$

where x and y represent the population densities of the prey and predator, respectively, and explored several bifurcations such as the saddle-node bifurcation, the supercritical Hopf bifurcation, and subcritical Hopf bifurcation occurring in system (1). Besides, Gong et al. [6] discussed the Bogdanov–Takens bifurcation of codimension 2 of system (1). On the basis of system (1), Huang et al. [9] introduced the Holling and Leslie-type functional response, and various kinds of bifurcation, including saddle-node, Hopf, Bogdanov–Takens bifurcation, were shown in the model. Biswas et al. [2] considered a modified Leslie–Gower prey–predator reaction–diffusion model introducing harvesting of both species. They found the stability regions and drawn bifurcation diagrams, and reveal that the harvesting has a stabilizing effect. Also, they showed that the temporal system appeared transcritical and Hopf bifurcations. Additionally, they determined Turing instability conditions for the spatiotemporal model and the amplitude equation for the critical modes. Bhutia et al. [1] proposed a modified form of the Rosenzweig–MacArthur model by incorporating prey harvesting and variable carrying capacity. They identified the sufficient criteria for the stability and occurrence of Hopf bifurcation. Also, they established the conditions for Turing instability and demonstrated that the system cannot produce heterogeneous spatial patterns without cross-diffusion. [5, 8] considered system (1) with different functional response or harvesting types, which exhibit more complex dynamic behaviors.

Aside from being directly captured, prey groups can also be indirectly consumed through factors like fear of predators. Furthermore, the collective anxiety within prey groups about survival can have a similar impact as being actively hunted. Essentially, the physiological condition of prey populations influenced by fear can play a role in system dynamics. Wang et al. [16] have taken fear factor into account in their study on the reproduction of prey species and have introduced a following predator–prey model based on this concept:

$$\begin{aligned} \dot{x} &= rxf(k,y)-dx-ax^2-cxy, \\ \dot{y} &= -my+cpxy, \end{aligned} \tag{2}$$

where $f(k,y) = 1/(1+ky)$ represents the fear function, which indicates the cost of antipredator defense of prey caused by fear from predator. Here k stands for the level of fear. Hence, in a biological context, the function $f(k,y)$ must meet the following criteria: $f(0,y)=1$, $f(k,0)=1$, $\lim_{k\to\infty} f(k,y)=0$, $\lim_{y\to\infty} f(k,y)=0$, $\partial f(k,y)/\partial k<0$, and $\partial f(k,y)/\partial y < 0$. They studied two models with varying functional responses and discovered that the fear effect does not alter the dynamics of the model with linear functional response (i.e., system (2)), but does affect the dynamics of the model with

Holling type II functional response. They observed that a strong fear effect leads to system stability, while a weak fear effect causes multiple limit cycles, resulting in a bistable phenomenon. Chen et al. [3] incorporated fear effect into Leslie–Gower predator–prey model and drew a conclusion that transcritical bifurcation, Hopf bifurcation, and Bogdanov–Takens bifurcation have taken place. Wang et al. [15] examined the concepts of refuge, fear effect, and harvesting within a Beddington–DeAngelis predator–prey model. They investigated the local stability of equilibria and looked into various bifurcations including saddle-node, transcritical, Hopf, and Bogdanov–Takens bifurcation. Additionally, the predator–prey systems with fear effect have been widely researched by numerous scholars [11, 14, 17].

In this paper, incorporating the fear effect into system (1) leads to the model below:

$$\begin{aligned} \dot{x} &= \frac{rx}{1+ky} - ax^2 - dx - cxy - h, \\ \dot{y} &= sy\left(1 - \frac{y}{nx}\right), \end{aligned} \tag{3}$$

where r is prey birthrate, d is prey natural mortality rate. Clearly, biologically speaking, $r > d$. a is intraspecific competition between prey, c is the predator's maximum predation rate, s is the predators' intrinsic growth rates, n is used to measure the quality of food provided by prey to predator, k is a parameter of fear, h is the constant-type prey harvesting. From a biological point of view, in the initial stage, if prey population is abundant, constant-type harvesting may not pose a great threat to prey population. However, as time passes, if the amount of harvesting exceeds the growth of the population, the population number will gradually decline, leading to changes in the population structure. The existence of fear effect will cause prey to exhibit behavioral changes to reduce the risk of being preyed upon such as reducing the range of activities and foraging time. Moreover, the fear effect forces prey to remain in a state of high alert for a long time, resulting in a shortening of the reproduction cycle and a reduction in the number of offspring, thus causing a decline in its population density.

In this article, we focus on the types of equilibria of system (3) as well as bifurcations that may occur in system (3). When system (3) has only one degenerate boundary equilibrium, it is an unstable saddle-node. When system (3) has two positive equilibria, one of them is a saddle and the other may be a weak focus of order 2, which indicates that system (3) undergoes degenerate Hopf bifurcation under appropriate parameters. When system (3) has only one degenerate positive equilibrium, we will prove that it may be a cusp of codimension 2, which indicates that system (3) undergoes Bogdanov–Takens bifurcation of codimension 2 under appropriate parameters.

For simplicity, letting

$$\begin{aligned} &\bar{x} = \frac{a}{d}x, \qquad \bar{y} = \frac{a}{dn}y, \qquad \bar{t} = dt, \qquad \bar{s} = \frac{s}{d}, \\ &\bar{c} = \frac{cn}{a}, \qquad \bar{h} = \frac{ah}{d^2}, \qquad \bar{r} = \frac{r}{d}, \qquad \bar{k} = \frac{kdn}{a} \end{aligned}$$

and dropping the bars, system (3) becomes

$$\begin{aligned} \dot{x} &= x\left(\frac{r}{1+ky} - x - 1 - cy\right) - h, \\ \dot{y} &= sy\left(1 - \frac{y}{x}\right), \end{aligned} \tag{4}$$

where $r > 1$, and r, k, c, s, h are positive constants.

The rest of this article will be structured in the following way. In Section 2, we give some conditions for boundary and positive equilibria to exist and examine the stability of these equilibria. In Section 3, we prove that system (4) undergoes a saddle-node bifurcation, Hopf bifurcation, and Bogdanov–Takens bifurcation of codimension 2. In Sections 4 and 5, some numerical simulations and conclusion are given.

2 Existence and stability of equilibria

2.1 Existence of equilibria

Conditions for boundary and positive equilibria of system (4) to exist are going to be investigated in this section.

The first step is to analyse whether a boundary equilibrium of system (4) exists. If $y = 0$, we can transform the first equation of system (4) into

$$\dot{x} = x(r - 1 - x) - h.$$

Let

$$f(x) = x^2 - (r-1)x + h,$$

whose discriminant is $\Delta_1 = (r-1)^2 - 4h$.

If $h > (r-1)^2/4$, then $f(x)$ has no positive roots. If $h = (r-1)^2/4$, then $f(x)$ has only one positive root $\bar{x} = (r-1)/2$. If $0 < h < (r-1)^2/4$, then $f(x)$ has two positive roots x_1 and x_2, where $x_{1,2} = (r - 1 \mp \sqrt{\Delta_1})/2$.

Hence, we get the following lemma regarding the presence of boundary equilibria in system (4).

Lemma 1. *The boundary equilibria of system* (4) *are present as outlined below*:

(i) *When* $h > (r-1)^2/4$, *system* (4) *has no boundary equilibrium*;
(ii) *When* $h = (r-1)^2/4$, *system* (4) *has a unique equilibrium* $\bar{E}(\bar{x}, 0)$;
(iii) *When* $0 < h < (r-1)^2/4$, *system* (4) *has two boundary equilibria* $E_1(x_1, 0)$ *and* $E_2(x_2, 0)$.

Next, is a discussion of whether positive equilibria exist in system (4). Notice that the positive equilibria satisfies

$$\frac{rx}{1+ky} - x - x^2 - cxy - h = 0, \qquad y = x.$$

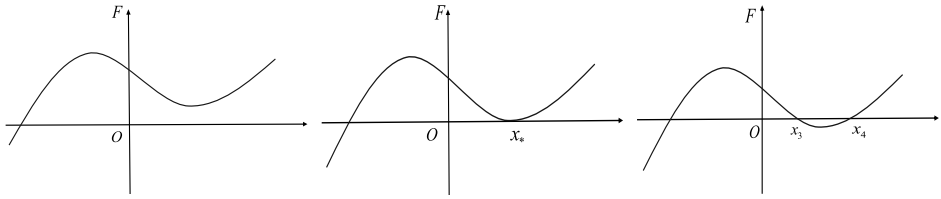

(a) (b) (c)

Figure 1. Roots of $F(x) = 0$ when $0 < h < (r-1)/k$: (a) $F(x_*) > 0$, no positive root; (b) $F(x_*) = 0$, one positive root; (c) $F(x_*) < 0$, two positive roots.

We denote

$$F(x) = k(c+1)x^3 + (1+c+k)x^2 + (hk+1-r)x + h$$

and

$$F'(x) = 3k(c+1)x^2 + 2(1+c+k)x + hk + 1 - r$$

with the discriminant of $F'(x)$ being $\Delta_2 = 4(c+k+1)^2 - 12k(1+c)(hk+1-r)$.

Noting that $F(0) = h > 0$, $F(x)$ does not have any positive roots if $h \geqslant (r-1)/k$. In the following discussion, we will focus solely on the scenario where $0 < h < (r-1)/k$.

As $F'(0) = hk - r + 1 < 0$, $F'(x)$ has a positive real root

$$x_* = \frac{-2(1+c+k) + \sqrt{\Delta_2}}{6k(1+c)}.$$

Notice that $F(r-1) > 0$ and $F'(r-1) > 0$. Thus, $F(x) = 0$ has no positive root if $F(x_*) > 0$ (see Fig. 1(a)), only one positive root x_* if $F(x_*) = 0$ (see Fig. 1(b)), and two positive roots x_3 and x_4 ($0 < x_3 < x_* < x_4$) if $F(x_*) < 0$ (see Fig. 1(c)).

In summary, we have the following lemma.

Lemma 2. *If $0 < h < (r-1)/k$, the positive equilibria of system* (4) *are as listed below*:

(i) *If $F(x_*) > 0$, system* (4) *has no positive equilibrium*;
(ii) *If $F(x_*) = 0$, system* (4) *has a unique positive equilibrium $E_*(x_*, x_*)$*;
(iii) *If $F(x_*) < 0$, system* (4) *has two positive equilibria $E_3(x_3, x_3)$ and $E_4(x_4, x_4)$.*

2.2 Stability of equilibria

First of all, we introduce the fact that all positive solutions of system (4) are bounded in the end.

Lemma 3. *All positive solutions of system* (4) *with initial values located in R^2_+ are bounded for all $t > 0$.*

Proof. From the first equation in system (4) we have $\dot{x} \leqslant x(r-1-x)$ for all $t > 0$. That means $\limsup_{t\to\infty} x(t) \leqslant r-1$. Then from the second equation in system (4) we get $\dot{y} \leqslant sy(1 - y/(r-1))$ for all $t > 0$. That means $\limsup_{t\to\infty} y(t) \leqslant r-1$. This completes the proof of Lemma 3. □

Now, the stability of equilibria of system (4) is under investigation. The Jacobian matrix of system (4) at $E(x,y)$ is

$$J_E = \begin{pmatrix} \frac{r}{1+ky} - 1 - 2x - cy & x\left(-\frac{rk}{(ky+1)^2} - c\right) \\ \frac{s\,y^2}{x^2} & s\left(1 - \frac{y}{x}\right) - \frac{sy}{x} \end{pmatrix},$$

and

$$\operatorname{Det} J_E = \frac{s(2k^2(1+c)x^3 + k(4c+k+4)x^2 + 2(c+k+1)x - r + 1)}{(1+kx)^2},$$

$$\operatorname{Tr} J_E = -\frac{k(c+2)x^2 + ((s+1)k + c + 2)x - r + s + 1}{1+kx}.$$

Letting $F(x) = 0$, we have

$$k = -\frac{cx^2 + x^2 - rx + x + h}{x(cx^2 + x^2 + x + h)}. \tag{5}$$

Substituting (5) into $F'(x)$ and $\operatorname{Det} J_E$, we get

$$\operatorname{Det} J_E = \frac{s(cx^2 + x^2 + x + h)}{rx} F'(x). \tag{6}$$

Theorem 1. *If $0 < h < (r-1)^2/4$, system* (4) *has two boundary equilibria E_1 and E_2. Furthermore, E_1 is a hyperbolic unstable node, and E_2 is a hyperbolic saddle.*

Proof. The Jacobian matrices of system (4) at these two boundary equilibria are, respectively,

$$J_{E_1} = \begin{pmatrix} \sqrt{\Delta_1} & -x_1(rk+c) \\ 0 & s \end{pmatrix} \quad \text{and} \quad J_{E_2} = \begin{pmatrix} -\sqrt{\Delta_1} & -x_2(rk+c) \\ 0 & s \end{pmatrix}.$$

Obviously, E_1 is a hyperbolic unstable node, and E_2 is a hyperbolic saddle. This completes the proof of Theorem 1. □

Theorem 2. *If $h = (r-1)^2/4$, system* (4) *has a unique boundary equilibrium $\bar{E}$, which is a repelling saddle-node.*

Proof. The Jacobian matrix of system (4) at $\bar{E}$ is

$$J_{\bar{E}} = \begin{pmatrix} 0 & -\frac{(r-1)(rk+c)}{s} \\ 0 & s \end{pmatrix},$$

where the eigenvalues of $J_{\bar{E}}$ are $\epsilon_1 = 0$ and $\epsilon_2 = s > 0$. To get the type of $\bar{E}$, we shift $\bar{E}$ to $(0,0)$ with the transformation $x = X + \bar{x}$, $y = Y$. Then system (4) is transformed into

the following form:

$$\begin{aligned} \dot{X} &= \acute{a}_{01}Y + \acute{a}_{20}X^2 + \acute{a}_{11}XY + \acute{a}_{02}Y^2 + o\big(|X,Y|^2\big), \\ \dot{Y} &= \acute{b}_{01}Y + \acute{b}_{02}Y^2 + o\big(|X,Y|^2\big), \end{aligned} \tag{7}$$

where $\acute{a}_{01} = -(r-1)(rk+c)/2$, $\acute{a}_{20} = -1$, $\acute{a}_{11} = -rk-c$, $\acute{a}_{02} = rk^2(r-1)/2$, $\acute{b}_{01} = s$, and $\acute{b}_{02} = -2s/(r-1)$.

Next, make the following transformation:

$$\begin{aligned} X &= -\frac{(rk+c)(r-1)}{2}u - \frac{(rk+c)(r-1)}{2}v, \\ Y &= sv, \qquad t = s\tau. \end{aligned}$$

Then system (7) can be written as

$$\begin{aligned} \dot{u} &= \acute{c}_{20}u^2 + \acute{c}_{11}uv + \acute{c}_{01}v^2 + o\big(|u,v|^2\big), \\ \dot{v} &= v + \acute{d}_{02}v^2 + o\big(|u,v|^2\big), \end{aligned} \tag{8}$$

where the coefficients of system (8) are omitted for brevity. From Theorem 7.1 in [21] we know that the equilibrium $\bar{E}$ is a repelling saddle-node for $c_{20} = (r-1)(kr+c)/(2s) > 0$. This completes the proof of Theorem 2. □

Theorem 3. *If condition* (iii) *of Lemma* 2 *holds, system* (4) *will possess two positive equilibria* $E_3(x_3, x_3)$ *and* $E_4(x_4, x_4)$*, where* E_3 *is a hyperbolic saddle. Moreover,*

(i) E_4 *is a stable node or focus if* $0 < h < x_4(s + x_4)$;
(ii) E_4 *is an unstable node or focus if* $h > x_4(s + x_4)$;
(iii) E_4 *is a center or weak focus if* $h = x_4(s + x_4)$.

Proof. From (6) we know that $\operatorname{Det} J_{E_3} < 0$ and $\operatorname{Det} J_{E_4} > 0$. Therefore, E_3 is always a hyperbolic saddle.

By computation we have $\operatorname{Tr} J_{E_4} = (h - x_4(s + x_4))/x_4$. If $h > x_4(s + x_4)$, then $\operatorname{Tr} J_{E_4} > 0$, that is, E_4 is an unstable node or focus; if $0 < h < x_4(s + x_4)$, then $\operatorname{Tr} J_{E_4} < 0$, that is, E_4 is a stable node or focus; if $h = x_4(s + x_4)$, then $\operatorname{Tr} J_{E_4} = 0$, that is, E_4 is a center or a weak focus. This completes the proof of Theorem 3. □

By setting $F(x_*) = 0$ and $F'(x_*) = 0$ we can express k and r in terms of x_*, s, h, and c as shown below:

$$k = \frac{h - (c+1)x_*^2}{x_*^2(2cx_* + 2x_* + 1)}, \qquad r = \frac{(cx_*^2 + 2x_*^2 + h + x_*)^2}{x_*^2(2cx_* + 2x_* + 1)}, \tag{9}$$

where $h > (c+1)x_*^2$ for the positivity of k and r.

The next theorem shows the dynamic behaviour of E_*.

Theorem 4. *Under the assumption that* (9) *holds, there is a unique positive equilibrium* $E_*(x_*, y_*)$ *in system* (4)*. Moreover,*

(i) *E_* is a saddle-node with a stable parabolic sector if $s > cx_*$ and $(c+1)x_*^2 < h < x_*(s+x_*)$;*

(ii) *E_* is a saddle-node with an unstable parabolic sector if $s \leqslant cx_*$ and $h > (c+1)x_*^2$, or $s > cx_*$ and $h > x_*(s+x_*)$.*

Proof. Based on (6) and $F'(x_*) = 0$, we can know $\operatorname{Det} J_{E_*} = 0$. Therefore, the stability of E_* relies on the sign of $\operatorname{Tr} J_{E_*}$, that is,

$$\operatorname{Tr} J_{E_*} = \frac{h - (x_* + s)x_*}{x_*}.$$

Firstly, make $(x, y) = (u + x_*,\ v + y_*)$, then system (4) can be written as

$$\begin{aligned} \dot{u} &= \hat{a}_{10}u + \hat{a}_{01}v + \hat{a}_{20}u^2 + \hat{a}_{11}uv + \hat{a}_{02}v^2 + o\big(|u, v|^2\big), \\ \dot{v} &= \hat{b}_{10}u + \hat{b}_{01}v + \hat{b}_{20}u^2 + \hat{b}_{11}uv + \hat{b}_{02}v^2 + o\big(|u, v|^2\big), \end{aligned} \tag{10}$$

where the coefficients of system (10) are omitted for brevity. It is obvious that the eigenvalues of the Jacobian matrix at E_* are $\epsilon_3 = 0$ and $\epsilon_4 = (h - (x_* + s)x_*)/x_*$. If $h \neq (x_* + s)x_*$, then $\epsilon_4 \neq 0$.

Next, by implementing the subsequent transformation

$$(u, v) = \left(X + Y,\ X + \frac{sx_*}{h - x_*^2}Y\right), \qquad \mathrm{d}\tau = \operatorname{Tr} J_{E_*}\,\mathrm{d}t$$

system (10) can be expressed as

$$\begin{aligned} \dot{X} &= \hat{c}_{20}X^2 + \hat{c}_{11}XY + \hat{c}_{02}Y^2 + o\big(|X, Y|^2\big), \\ \dot{Y} &= Y + \hat{d}_{20}X^2 + \hat{d}_{11}XY + \hat{d}_{02}Y^2 + o\big(|X, Y|^2\big), \end{aligned} \tag{11}$$

where the coefficients of system (11) are omitted for brevity.

Through conducting calculations, we get

$$\hat{c}_{20} = \frac{sx_*M}{(h - sx_* - x_*^2)^2(cx_*^2 + x_*^2 + x_* + h)},$$

where $M = (1 + 3x_* + 3cx_*)h - (c+1)^2x_*^3$. Note that $h \neq (x_* + s)x_*$ as $\operatorname{Tr} J_{E_*} \neq 0$. Thus, the sign of $\hat{c}_{20}$ depends on M. Through computation, we get

$$M|_{h=(c+1)x_*^2} = (c+1)(2cx_* + 2x_* + 1)x_*^2,$$

which means $M > 0$ for $h > (c+1)x_*^2$. Thus, $\hat{c}_{20} > 0$ for $h > (c+1)x_*^2$.

Notice that $x_*(s+x_*) - (c+1)x_*^2 = x_*(s - cx_*)$. Considering a time transformation and applying Theorem 7.1 in [21], if $s > cx_*$ and $(c+1)x_*^2 < h < x_*(s+x_*)$, we have $\operatorname{Tr} J_{E_*} < 0$, then E_* is a saddle-node with a stable parabolic sector; see Fig. 2(a). If $s \leqslant cx_*$ and $h > (c+1)x_*^2$ or $s > cx_*$ and $h > x_*(s+x_*)$, we have $\operatorname{Tr} J_{E_*} > 0$, then E_* is a saddle-node with an unstable parabolic sector; see Fig. 2(b). This completes the proof of Theorem 4. □

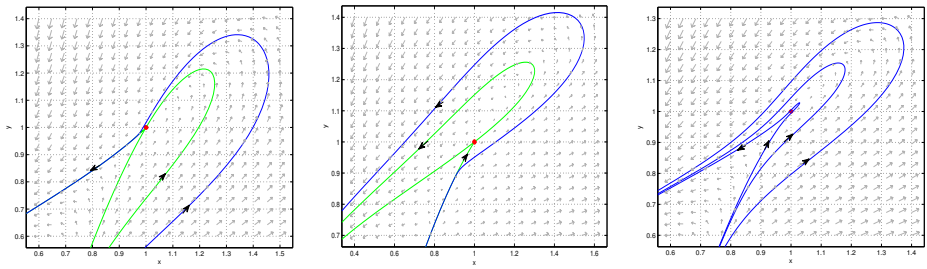

(a) (b) (c)

Figure 2. Phase portraits of system (4): (a) E_* is a saddle-node with attracting parabolic with $c = 1$, $s = 2$, $h = 2.2$, $k = 0.04$, and $r = 5.408$; (b) E_* is a saddle-node with repelling parabolic with $c = 1$, $s = 2$, $h = 5$, $k = 0.6$, and $r = 12.8$; (c) E_* is a cusp of codimension 2 with $c = 1$, $s = 1.5$, $h = 2.5$, $k = 0.1$, and $r = 6.05$.

If $h = (x_* + s)x_*$, then $\operatorname{Tr} J_{E_*} = 0$. By setting $F(x_*) = F'(x_*) = \operatorname{Tr} J_{E_*} = 0$ we can represent h, k, and r in terms of x_*, s, and c as shown below:

$$h = x_*(s + x_*), \qquad k = \frac{s - cx_*}{x_*(1 + 2x_* + 2cx_*)}, \qquad r = \frac{(1 + s + 2x_* + cx_*)^2}{1 + 2x_* + 2cx_*}, \tag{12}$$

where $s > cx_*$.

Using the following lemma, we show that E_* is a cusp of codimension 2.

Theorem 5. *Assume that* (12) *and* $s > cx_*$ *hold, then* E_* *is a cusp of codimension 2.*

Proof. Letting $u = x - x_*$ and $v = y - y_*$, system (10) can be rewritten as

$$\begin{aligned} \dot{u} &= su - sv - u^2 - \frac{s}{x_*}uv + \frac{(s - cx_*)^2}{x_*(1 + s + cx_* + 2x_*)}v^2 + o\big(|u, v|^2\big), \\ \dot{v} &= su - su - \frac{s}{x_*}u^2 + \frac{2s}{x_*}uv - \frac{s}{x_*}v^2 + o\big(|u, v|^2\big). \end{aligned} \tag{13}$$

By the transformation $(X, Y) = (-u/s,\ -u + v)$ system (13) becomes

$$\begin{aligned} \dot{X} &= Y + \tilde{e}_{20}X^2 + \tilde{e}_{11}XY + \tilde{e}_{02}Y^2 + o\big(|X, Y|^2\big), \\ \dot{Y} &= \tilde{f}_{20}X^2 + \tilde{f}_{11}XY + \tilde{f}_{02}Y^2 + o\big(|X, Y|^2\big), \end{aligned} \tag{14}$$

where the coefficients of system (14) are omitted for brevity. By Lemma 1 in [9] system (14) is equivalent to

$$\dot{x} = y, \qquad \dot{y} = \tilde{f}_{20}x^2 + (\tilde{f}_{11} + 2\tilde{e}_{20})xy + o\big(|x, y|^2\big).$$

Obviously, $\tilde{f}_{11} + 2\tilde{e}_{20} = s(s + 2x_*)/x_* \neq 0$. Substituting $s = cx_*$ into T_1, we have

$$T_1|_{s=cx_*} = -x_*\big(2c^2x_* + 4cx_* + 2x_* + c + 1\big).$$

Thus, $T_1 < 0$ for $s > cx_*$, that is, $\tilde{f}_{20} \neq 0$ for $s > cx_*$. Hence, according to [13], E_* is a cusp of codimension 2 as illustrated in Fig. 2(c). This completes the proof of Theorem 5. □

3 Bifurcation

In this section, we will prove that system (4) is capable of undergoing three types of bifurcations: saddle-node bifurcation, Hopf bifurcation, and Bogdanov–Takens bifurcation.

3.1 Saddle-node bifurcation

According to Lemma 1 and Theorem 2, when $h = (r-1)^2/4$, system (4) has a single boundary equilibrium $\bar{E}((r-1)/2, 0)$, which is a saddle-node. By changing the parameter h from $0 < h < (r-1)^2/4$ to $h > (r-1)^2/4$ (or vice versa) the quantity of boundary equilibria of system (4) transitions from two to zero (or from zero to two). Hence, based on Sotomayor's theorem [13], it can be concluded that system (4) undergoes a saddle-node bifurcation at $\bar{E}$.

Theorem 6. *When h crosses the critical value $h_{\mathrm{SN}} = (r-1)^2/4$, system* (4) *undergoes a saddle-node bifurcation at $\bar{E}$.*

Proof. The Jacobian matrix of system (4) at $\bar{E}$ is

$$J(\bar{E}; h_{\mathrm{SN}}) = \begin{pmatrix} 0 & -\frac{(r-1)(rk+c)}{2} \\ 0 & s \end{pmatrix}.$$

Then $J(\bar{E}; h_{\mathrm{SN}})$ has a zero eigenvalue. Let V and W be the eigenvectors corresponding to the zero eigenvalue of $J(\bar{E}; h_{\mathrm{SN}})$ and $J(\bar{E}; h_{\mathrm{SN}})^T$, respectively. Choose

$$V = \begin{pmatrix} V_1 \\ V_2 \end{pmatrix} = \begin{pmatrix} 1 \\ 0 \end{pmatrix} \quad \text{and} \quad W = \begin{pmatrix} W_1 \\ W_2 \end{pmatrix} = \begin{pmatrix} 1 \\ \frac{(r-1)(rk+c)}{2s} \end{pmatrix}.$$

Define

$$F(x, y) = \begin{pmatrix} F_1(x, y) \\ F_2(x, y) \end{pmatrix} = \begin{pmatrix} x(\frac{r}{1+ky} - 1 - x - cy) - h \\ sy(1 - \frac{y}{x}) \end{pmatrix}.$$

Hence,

$$F_h(\bar{E}, h_{\mathrm{SN}}) = \begin{pmatrix} -1 \\ 0 \end{pmatrix},$$

$$D^2F(\bar{E}; h_{\mathrm{SN}})(V, V) = \begin{pmatrix} \frac{\partial^2 F_1}{\partial x^2}V_1^2 + 2\frac{\partial^2 F_1}{\partial x \partial y}V_1V_2 + \frac{\partial^2 F_1}{\partial y^2}V_2^2 \\ \frac{\partial^2 F_2}{\partial x^2}V_1^2 + 2\frac{\partial^2 F_2}{\partial x \partial y}V_1V_2 + \frac{\partial^2 F_2}{\partial y^2}V_2^2 \end{pmatrix}_{(\bar{E}; h_{\mathrm{SN}})} = \begin{pmatrix} -2 \\ 0 \end{pmatrix}.$$

Therefore, it is easily seen that V and W meet the following transversality conditions:

$$W^T F_h(\bar{E}; h_{\mathrm{SN}}) = -1 \neq 0, \qquad W^T \left[D^2F(\bar{E}; h_{\mathrm{SN}})(V, V)\right] = -2 \neq 0.$$

Hence, system (4) undergoes a saddle-node bifurcation around $\bar{E}$ at $h = h_{\mathrm{SN}}$. This completes the proof of Theorem 6. □

Similarly, from Lemma 2 we know that system (4) undergoes a saddle-node bifurcation around E_*.

Theorem 7. *Assume that $0 < h < (r-1)/k$ and $F(x_*) = 0$, then system* (4) *will undergo a saddle-node bifurcation at E_*.*

3.2 Hopf bifurcation

According to Theorem 3, the stability of E_4 will vary with fluctuations in the parameter h. If $h = x_4(s+x_4)$, then E_4 is a center or a weak focus, meaning the eigenvalues of J_{E_4} will be a pair of imaginary roots. Thus, Hopf bifurcation will occurs at E_4. For simplicity, inspired by the method in Dai et al. [4] and Lu et al. [12], letting

$$\bar{x} = \frac{x}{x_4}, \qquad \bar{y} = \frac{y}{y_4}, \qquad \bar{t} = x_4 t, \qquad \bar{r} = \frac{r}{x_4}, \qquad \bar{k} = x_4 k,$$
$$\bar{a} = \frac{1}{x_4}, \qquad \bar{c} = c, \qquad \bar{h} = \frac{h}{x_4^2}, \qquad \bar{s} = \frac{s}{x_4}$$

and dropping the bar, system (4) is transformed to the following system:

$$\dot{x} = x\left(\frac{r}{ky+1} - a - x - cy\right) - h, \qquad \dot{y} = sy\left(1 - \frac{y}{x}\right), \tag{15}$$

where $r > a > 0$, and all the other parameters are positive.

$\tilde{E}_4(1,1)$ is an equilibrium of system (15), which implies that

$$r = (a + 1 + c + h)(k + 1).$$

Assume that there is another positive equilibrium $\tilde{E}_3(\tilde{x}_3, \tilde{x}_3)$ with $\tilde{x}_3$ satisfying the equation

$$(x-1)\Phi(x) = 0,$$

where

$$\Phi(x) = k(c+1)x^2 + \big(ak + (k+1)(c+1)\big)x - h.$$

Note that $\tilde{x}_3 < 1$. Substituting $x = 1$ into $\Phi(x)$, we have $\Phi(1) = h_* - h > 0$, that means $h < h_*$, where $h_* = (2k+1)(c+1) + ak$.

The Jacobian matrix of system (15) at $\tilde{E}_4$ is

$$J_{\tilde{E}_4} = \begin{pmatrix} -1 + h & \frac{(a+2c+h+1)k+c}{k+1} \\ s & -s \end{pmatrix},$$

and

$$\operatorname{Det} J_{\tilde{E}_4} = \frac{s(h_* - h)}{k+1}, \qquad \operatorname{Tr} J_{\tilde{E}_4} = h - h_{**},$$

where $h_{**} = s + 1$.

Theorem 8. *Assuming that $h < h_*$, system* (15) *has an equilibrium $\tilde{E}_4(1,1)$. Moreover,*

(i) *$\tilde{E}_4(1,1)$ is a stable node or a focus if $h < h_{**}$;*
(ii) *$\tilde{E}_4(1,1)$ is an unstable node or a focus if $h > h_{**}$;*
(iii) *$\tilde{E}_4(1,1)$ is a center or a weak focus if $h = h_{**}$.*

Now we will be going to study the Hopf bifurcation around $\tilde{E}_4(1,1)$ in system (15). It is clear that the condition of transversality

$$\left.\frac{\mathrm{d}\operatorname{Tr} J_{\tilde{E}_4}}{\mathrm{d}h}\right|_{h=h_{**}} = 1 \neq 0$$

holds. Then we will calculate the first-order Lyapunov number to assess the stability of the limit cycle around $\tilde{E}_4$. Applying the transformations $(\tilde{x}, \tilde{y}) = (x-1, y-1)$, the Taylor series expansion of system (15) around the origin can be expressed as

$$\begin{aligned}\dot{\tilde{x}} &= \tilde{a}_{10}\tilde{x} + \tilde{a}_{01}\tilde{y} + \tilde{a}_{20}\tilde{x}^2 + \tilde{a}_{11}\tilde{x}\tilde{y} + \tilde{a}_{02}\tilde{y}^2 + \tilde{a}_{30}\tilde{x}^3 + \tilde{a}_{21}\tilde{x}^2\tilde{y} + \tilde{a}_{12}\tilde{x}\tilde{y}^2 + \tilde{a}_{03}\tilde{y}^3 \\ &\quad + o\big(|\tilde{x}, \tilde{y}|^3\big), \\ \dot{\tilde{y}} &= \tilde{b}_{10}\tilde{x} + \tilde{b}_{01}\tilde{y} + \tilde{b}_{20}\tilde{x}^2 + \tilde{b}_{11}\tilde{x}\tilde{y} + \tilde{b}_{02}\tilde{y}^2 + \tilde{b}_{30}\tilde{x}^3 + \tilde{b}_{21}\tilde{x}^2\tilde{y} + \tilde{b}_{12}\tilde{x}\tilde{y}^2 + \tilde{b}_{03}\tilde{y}^3 \\ &\quad + o\big(|\tilde{x}, \tilde{y}|^3\big),\end{aligned} \tag{16}$$

where the coefficients of system (16) are omitted for brevity.

Next, applying the transformation $(\tilde{u}, \tilde{v}) = (-\tilde{x}, (\tilde{a}_{10}\tilde{x} + \tilde{a}_{01}\tilde{y})/\sqrt{D})$, where $D = \tilde{a}_{10}\tilde{b}_{01} - \tilde{a}_{01}\tilde{b}_{10} = \operatorname{Det} J_{\tilde{E}_4} > 0$, system (16) is modified to

$$\begin{aligned}\dot{\tilde{u}} &= -\sqrt{D}\tilde{v} + \tilde{c}_{20}\tilde{u}^2 + \tilde{c}_{11}\tilde{u}\tilde{v} + \tilde{c}_{02}\tilde{v}^2 + \tilde{c}_{30}\tilde{u}^3 + \tilde{c}_{21}\tilde{u}^2\tilde{v} + \tilde{c}_{12}\tilde{u}\tilde{v}^2 + \tilde{c}_{03}\tilde{v}^3 \\ &\quad + o\big(|\tilde{u}, \tilde{v}|^3\big), \\ \dot{\tilde{v}} &= \sqrt{D}\tilde{u} + \tilde{d}_{20}\tilde{u}^2 + \tilde{d}_{11}\tilde{u}\tilde{v} + \tilde{d}_{02}\tilde{v}^2 + \tilde{d}_{30}\tilde{u}^3 + \tilde{d}_{21}\tilde{u}^2\tilde{v} + \tilde{d}_{12}\tilde{u}\tilde{v}^2 + \tilde{d}_{03}\tilde{v}^3 \\ &\quad + o\big(|\tilde{u}, \tilde{v}|^3\big),\end{aligned} \tag{17}$$

where the coefficients of system (17) are omitted are omitted for brevity.

On the basic of the result of [21], the first-order Lyapunov number can be expressed as

$$l_1 = \frac{\gamma_1 k^2 + \gamma_2 k + \gamma_3}{8((a+2c+s+2)k+c)(1+k)D},$$

where the expression of γ_i $(i = 1, 2, 3)$ are omitted for brevity.

Theorem 9. *If $h = h_{**} < h_*$, then the following statements hold*:

(i) *If $l_1 > 0$, then system* (15) *undergoes a subcritical Hopf bifurcation, and an unstable limit cycle comes out around $\tilde{E}_4$*;

(ii) *If $l_1 < 0$, then system* (15) *undergoes a supercritical Hopf bifurcation, and a stable limit cycle comes out around $\tilde{E}_4$*;

(iii) *If $l_1 = 0$, then system* (15) *undergoes a degenerate Hopf bifurcation, and multiple limit cycles may appear around $\tilde{E}_4$.*

By numerical simulation we show the existence of limit cycle. Letting $a = 1$, $c = 0.6$, $s = 0.2$, $k = 0.1$, $h = 1.2$, $r = 4.18$, we have $l_1 = 0.3152321764 > 0$. We perturb h to $h = 1.2 - 0.01$, then there exists an unstable limit cycle around $\tilde{E}_4$; see Fig. 3(a)). On the other hand, letting $a = 1$, $c = 1.4$, $s = 0.2$, $k = 0.6$, $h = 1.2$, $r = 7.36$, we have $l_1 = -0.01607179488 < 0$. We perturb h to $h = 1.2 + 0.0029$, then there exists an stable limit cycle around $\tilde{E}_4$; see Fig. 3(b).

Now we give an example to illustrate the existence of two limit cycles. Letting $a = 1$, $c = 13/2$, $s = 5/2$, $k = (863 + 6\sqrt{39646})/1117$, $h = 7/2$, $r = (23760 + 72 \times \sqrt{39646})/1117$, where $l_1 = 0$, we perturb h and s to $h = 7/2 + 0.008$ and $s = 5/2 + 0.006$. Hence, system (15) undergoes a degenerates Hopf bifurcation, and there are two limit cycles (the inner one is stable, and the outer one is unstable) around $\tilde{E}_4$; see Fig. 3(c).

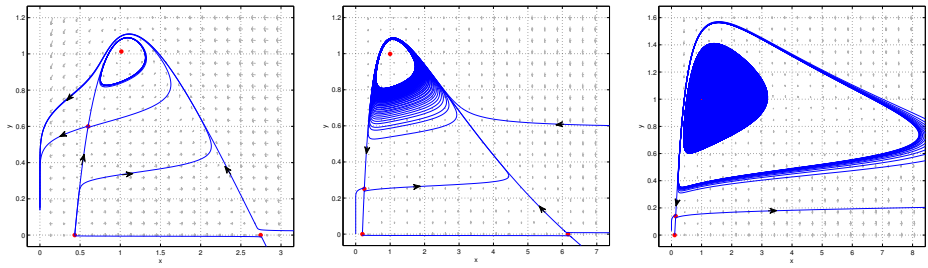

(a) (b) (c)

Figure 3. Limit circles of system (15): (a) an unstable limit cycle with $a = 1$, $c = 0.6$, $k = 0.1$, $h = 1.2 - 0.01$, $s = 0.2$, and $r = 4.18$; (b) a stable limit cycle appears with $a = 1$, $c = 1.4$, $k = 0.6$, $h = 1.2 + 0.0029$, $s = 0.2$, and $r = 7.36$; (c) two limit cycles (the inner one is stable, while the outer is unstable) with $a = 1$, $c = 13/2$, $k = (863 + 6\sqrt{39646})/1117$, $h = 7/2 + 0.008$, $s = 5/2 + 0.006$, and $r = (23760 + 72\sqrt{39646})/1117$.

Remark 1. In Fig. 3(a), the origin is stable, and one boundary equilibria is a unstable node, while another is a saddle. What is more, there are two positive equilibrium, where $\tilde{E}_3$ is a saddle, and $\tilde{E}_4$ is a stable focus, and a unstable limit cycle appears around $\tilde{E}_4$. The orbits of phase portraits reveal that the prey and predator tend to coexistent steady states only when initial values of system (15) lie inside of the unstable limit cycle; otherwise, the two species turn to die out.

In Fig. 3(b), except $\tilde{E}_4$ becomes a unstable focus, the origin and the other equilibrium remain the same. Besides, a stable limit cycle appears around $\tilde{E}_4$. When the initial values lies on the right of the two stable invariant manifolds of the saddle, the two species tend to coexistent, while when the initial values lies on the left of the two stable invariant manifolds of the saddle, the two species tend to die out.

In Fig. 3(c), we can know that system (15) undergoes degenerate Hopf bifurcation, and there appear two limit cycles (the inner one is stable, while the outer is unstable). That is, the two species will coexistent if the initial value is inside of the unstable limit cycle, otherwise both will die out.

3.3 Bogdanov–Takens bifurcation

According to Theorem 5, the unique positive equilibrium E_* of system (4) is a cusp of codimension 2, indicating the possibility of a Bogdanov–Takens bifurcation occurring near E_*. Thus, choosing s and k as the bifurcation parameters, system (4) transforms into

$$\begin{aligned} \dot{x} &= x\left(\frac{r}{1+(k+\lambda_1)y} - 1 - x - cy\right) - h, \\ \dot{y} &= (s+\lambda_2)y\left(1 - \frac{y}{x}\right), \end{aligned} \tag{18}$$

where the parameter vector (λ_1, λ_2) is located in a small vicinity around the origin.

Theorem 10. *Assume that the conditions of Theorem* 5 *hold, then system* (4) *undergoes a Bogdanov–Takens bifurcation of codimension 2 around* E_*.

Proof. First, perform the following transformations in sequence:

$$\begin{aligned} &x_1 = x - x_*, && y_1 = y - y_*, \\ &x_2 = y_1, && y_2 = \tilde{h}_{10}x_1 + \tilde{h}_{01}y_1 + \tilde{h}_{20}x_1^2 + \tilde{h}_{11}x_1y_1 + \tilde{h}_{02}y_1^2, \\ &x_3 = x_2, && y_3 = y_2(1 - \tilde{j}_{02}x_2), \qquad \mathrm{d}t = (1 - \tilde{j}_{02}x_2)\,\mathrm{d}\tau. \end{aligned}$$

Then system (18) is restated as (still denote τ as t)

$$\begin{aligned} &\dot{x}_3 = y_3, \\ &\dot{y}_3 = \tilde{k}_{00} + \tilde{k}_{10}x_3 + \tilde{k}_{01}y_3 + \tilde{k}_{20}x_3^2 + \tilde{k}_{11}x_3y_3 + o\big(|x_3, y_3|^2\big), \end{aligned} \tag{19}$$

where the coefficients system (19) are omitted for brevity.

Since $s > cx_*$, we get

$$\tilde{k}_{20}|_{\lambda_1=\lambda_2=0} = \frac{sT_1}{x_*(1 + s + cx_* + 2x_*)} < 0,$$

where T_1 is defined in Theorem 5. Letting

$$x_4 = x_3, \qquad y_4 = \frac{y_3}{\sqrt{-\tilde{k}_{20}}}, \qquad \tau = \sqrt{-\tilde{k}_{20}}t,$$

system (19) transforms into the following form:

$$\begin{aligned} &\dot{x}_4 = y_4, \\ &\dot{y}_4 = \tilde{m}_{00} + \tilde{m}_{10}x_4 + \tilde{m}_{01}y_4 - x_4^2 + \tilde{m}_{11}x_4y_4 + o\big(|x_4, y_4|^2\big), \end{aligned} \tag{20}$$

where the coefficients system (20) are omitted for brevity.

Next, let

$$x_5 = x_4 - \frac{\tilde{m}_{10}}{2}, \qquad y_5 = y_4,$$

then system (20) can be transformed into the following system:

$$\begin{aligned} &\dot{x}_5 = y_5, \\ &\dot{y}_5 = \tilde{n}_{00} + \tilde{n}_{01}y_5 - x_5^2 + \tilde{n}_{11}x_5y_5 + o(|x_5, y_5|^2), \end{aligned} \tag{21}$$

where the coefficients system (21) are omitted for brevity. According to the proof of Theorem 5, we obtain

$$\tilde{n}_{11}|_{\lambda_1=\lambda_2=0} = -\sqrt{-\frac{(2x_* + s)^2(1 + s + 2x_* + cx_*)}{sx_*T_1}} < 0.$$

Finally, let

$$x_6 = -\tilde{n}_{11}^2x_5, \qquad y_6 = -\tilde{n}_{11}^3y_5, \qquad \tau = -\frac{1}{\tilde{n}_{11}}t.$$

The universal unfolding of system (18) is given by

$$\dot{x}_6 = y_6, \qquad \dot{y}_6 = \mu_1 + \mu_2 y_6 + x_6^2 + x_6 y_6 + o\big(|x_6, y_6|^2\big),$$

where $\mu_1 = -\tilde{n}_{00}\tilde{n}_{11}^4$, $\mu_2 = -\tilde{n}_{01}\tilde{n}_{11}$.

Note that

$$\left|\frac{\partial(\mu_1,\mu_2)}{\partial(\mu_1,\mu_2)}\right|_{\lambda_1=\lambda_2=0} = -\frac{x_*(cx_*+2x_*+s+1)^4(2x_*+s)^5(cx_*+2x_*+1)}{s^3T_1^4} \neq 0.$$

Based on research by Preko [13], when (λ_1, λ_2) is close to $(0, 0)$, system (4) undergoes a Bogdanov–Takens bifurcation of codimension 2. This completes the proof of Theorem 10. □

4 Numerical simulations

This paper considers a Leslie–Gower predator–prey model incorporating fear effect and constant-type harvesting in prey. The main factors influencing the dynamic behaviour of system (4) are fear of predators and harvesting. Numerical simulations show that the impact of constant-type harvest and fear effect on the dynamic behaviour of (4) are as follows.

4.1 The impact of fear effect

First of all, there is a discussion regarding the influence of fear effect. From Fig. 3 it can be seen that as the parameter k decreases, the number of positive equilibria of system (4) alters, resulting in the emergence of a saddle-node bifurcation. Furthermore, system (4) undergoes a Hopf bifurcation as shown in Fig. 3. For instance, allowing $(r_1, c_1, s_1, k_1, h_1) = (8.36, 3.8, 0.81, 0.1, 1.8)$ and $(r_2, c_2, s_2, k_2, h_2) = (10.488, 3.8, 0.8, 0.38, 1.8)$ and by calculation, the first-order Lyapunov number is as follows: $L_1|_{(r,c,s,k,h)=(r_1,c_1,s_1,k_1,h_1)} = 0.04462864722$ and $L_1|_{(r,c,s,k,h)=(r_2,c_2,s_2,k_2,h_2)} = -0.006671445061$. This implies that system (4) undergoes a subcritical Hopf bifurcation and a supercritical Hopf bifurcation, respectively.

To further investigate the effects of constant-type harvesting, we provide additional clarification regarding Fig. 4(b). When $k = 1.2$, system (4) has no positive equilibrium. Both predator and prey cannot coexist; see Fig. 5(a). When $k = 1.0390744$, system (4) has only one positive equilibrium, which is a saddle-node with unstable parabolic; see Fig. 5(b). When $k = 0.6$, system (4) has two positive equilibria, one being a saddle, and the other an unstable focus. According to Fig. 5(c), it can be observed that both the predator and prey species are unable to coexist. When $k = 0.3797$, there exist two limit cycles around the unstable focus with the inner one being stable and the outer one being unstable; see Fig. 5(d). When $k = 0.378$, there is a transition from an unstable state to a stable state for focus accompanied by the emergence of an unstable limit cycle around it. From Figs. 5(d) and 5(e) the unstable limit cycle can be regarded as a separatrix curve. It is only when the initial value lies within the unstable limit cycle thatthe predator

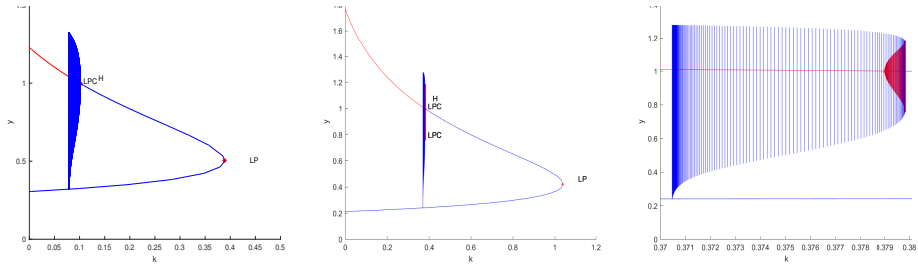

(a) (b) (c)

Figure 4. Bifurcation diagram of system (4) in k, y-plane: (a) $(r, c, s, h) = (r_1, c_1, s_1, h_1)$; (b) $(r, c, s, h) = (r_2, c_2, s_2, h_2)$. (c) The local amplified phase portrait of (b).

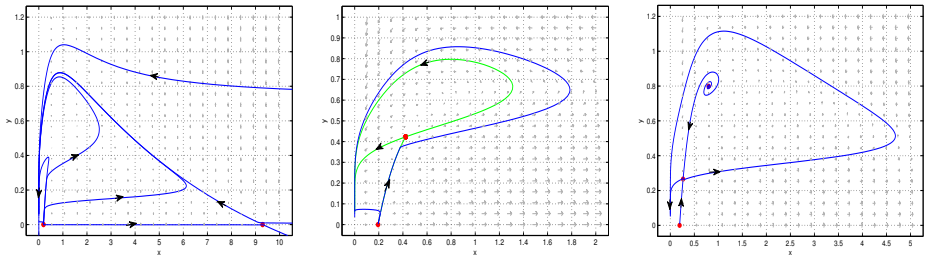

(a) $k = 1.2$ (b) $k = 1.0390744$ (c) $k = 0.6$

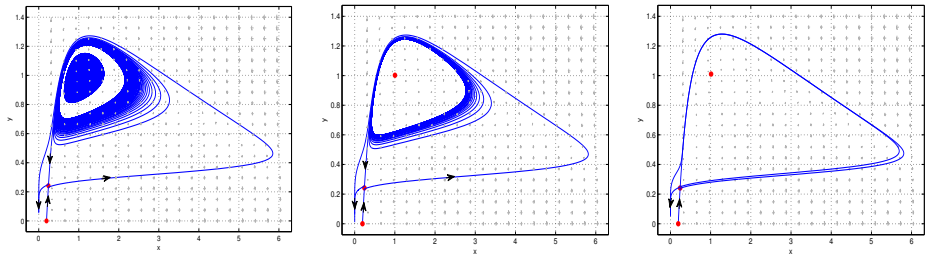

(d) $k = 0.3797$ (e) $k = 0.378$ (f) $k = 0.37058$

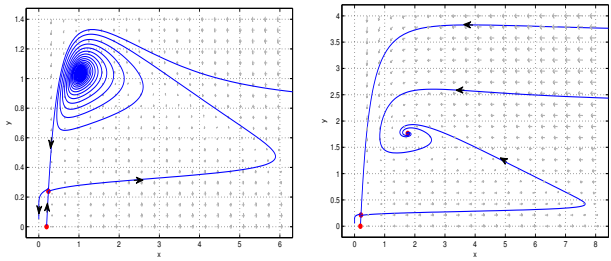

(g) $k = 0.35$ (h) $k = 0$

Figure 5. Phase portraits of system (4) with $(r, c, s, h) = (r_2, c_2, s_2, h_2)$.

and prey can coexist in a steady state or in periodic orbits. When $k = 0.37058$, the unstable limit cycle goes bigger and becomes a homoclinic loop finally; see Fig. 5(f). When $k = 0.35$, the unstable homoclinic disappears, and the focus remains stable. From Fig. 5(g) the two stable saddle manifolds serve as a separatrix curve, furthermore, prey and predator will be coexist if the initial value is to the right of the stable saddle manifolds, but will not coexist if the initial value is to the left of the stable saddle manifolds. When $k = 0$, the dynamic behaviors of system (4) shown in Fig. 5(h) is similar to that shown in Fig. 5(g). Figure 5 displays that when the fear effect is small, both predator and prey will survive or die out. But as the fear effect gradually increase, the area in which the species live together will decrease, and ultimately make it impossible for the coexistence of prey and predator. Therefore, the survival of both prey and predators is adversely affected by high levels of fear.

4.2 The impact of constant-type harvesting

Secondly, it discusses how constant harvesting is affected. Figure 6 shows that system (4) will undergo a Hopf bifurcation. Let $(r_3, c_3, s_3, k_3, h_3) = (12.6, 4.2, 1.8, 0.4, 2.8)$, $(r_4, c_4, s_4, k_4, h_4) = (11.34, 4.2, 0.9, 0.4, 1.9)$, and the first-order Lyapunov number as follows: $L_1|_{(r,c,s,k,h)=(r_3,c_3,s_3,k_3,h_3)} = 0.1238687618$ and $L_1|_{(r,c,s,k,h)=(r_4,c_4,s_4,k_4,h_4)} = -0.008220336145$, which means that system (4) undergoes a subcritical or a supercritical Hopf bifurcation, respectively.

From Figs. 7(a)–7(c) it can be observed that when the level of harvesting is high, it is not possible for both the prey and predator to coexist. From Figs. 7(d)–7(e) it can be seen that there exist two limit cycles with the inner one being stable and the outer one being unstable or one unstable limit cycle. In addition, the unstable limit cycle acts as a separatrix curve, allowing for the potential coexistence or absence of predator and prey depending on whether the initial value falls within or outside of the cycle. Figure 7(f) shows that the unstable limit cycle gets bigger and becomes a homoclinic loop. Figure 7(g) shows that the homoclinic loop disappears, and if the initial value is to the right of the stable saddle manifolds, prey and predator can coexist in a steady state. When

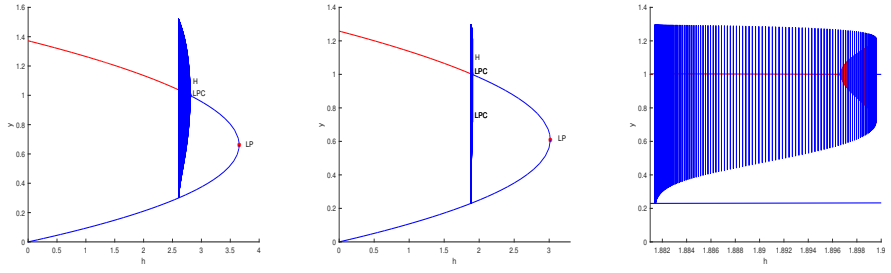

(a) (b) (c)

Figure 6. Bifurcation diagram of system (4) in h, y-plane: (a) $(r, c, s, k) = (r_3, c_3, s_3, k_3)$; (b) $(r, c, s, k) = (r_4, c_4, s_4, k_4)$. (c) The local amplified phase portrait of (b).

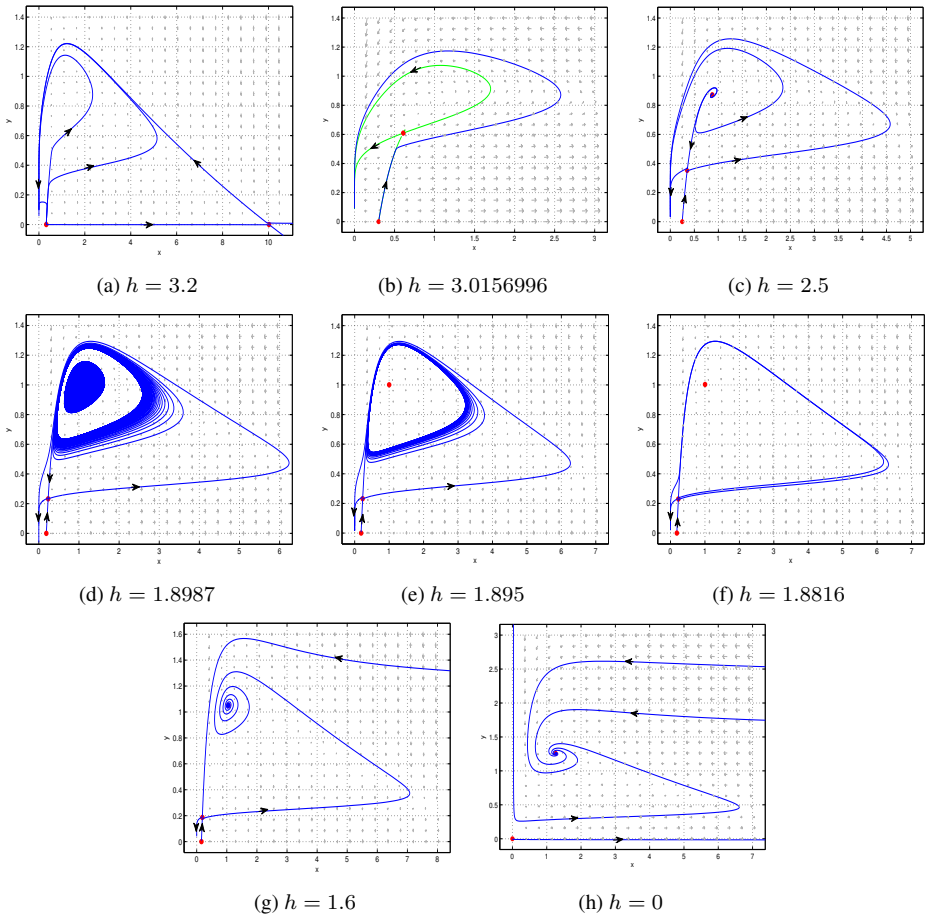

(a) $h = 3.2$ (b) $h = 3.0156996$ (c) $h = 2.5$

(d) $h = 1.8987$ (e) $h = 1.895$ (f) $h = 1.8816$

(g) $h = 1.6$ (h) $h = 0$

Figure 7. Phase portraits of system (4) with $(r, c, s, k) = (r_4, c_4, s_4, k_4)$.

$h = 0$, system (4) without constant-type harvesting has a single positive equilibria that is globally asymptotically stable; see Fig. 7(h). Figure 7 displays that excessive harvesting negatively impacts the survival of both prey and predator, highlighting the importance of implementing sustainable harvesting practices to ensure the survival of both species.

5 Conclusion

Qualitative analysis suggests that prey harvesting and fear of predators are key determinants of the dynamic behaviour of system (4). We get that the number and stability of boundary equilibrium for system (4) may change by the change of parameter h. Besides, the number of positive equilibrium for system (4) will vary by 0, 1, and 2 when there is minimal prey harvesting or fear effects, and so does their stability. We demonstrate

that, for a suitable range of parameters, the sole positive equilibrium E_* may be a saddle-node or a cusp of codimension 2. In addition, it is confirmed that saddle-node bifurcation and Bogdanov–Takens bifurcation occur around E_*, and expressions for three bifurcation curves are given, which consist of the saddle-node bifurcation curve, homoclinic bifurcation curve, and Hopf bifurcation curve. Furthermore, E_3 is consistently a saddle, whereas E_4 can be either stable or unstable depending on the parameter values. Additionally, system (4) undergoes a supercritical and subcritical Hopf bifurcation along with a degenerate Hopf bifurcation, resulting in the presence of two limit cycles with the inner one being stable and the outer one being unstable.

In [22], the authors studied the properties of the positive equilibrium and proved that supercritical or subcritical Hopf bifurcations and limit cycles occur in system (1). In [6], the authors further proved that system (1) can generate Bogdanov–Takens bifurcation of codimension 2. Different from [22] and [6], we demonstrates that the quantity of limit cycles can vary by zero, one (an unstable limit cycle), or two (with the inner one being stable and the outer one being unstable) within specific parameter ranges. That is, by choosing the suitable parameters we find system (4) to undergo a degenerate Hopf bifurcation, which is not discussed in [22] and [6]. In the realm of biology, the act of prey harvesting and fear of predator hold substantial significance, impacting the quantity and stability of equilibria as well as the occurrence of different bifurcations. Two species will attain a steady state only if the fear effect or prey harvesting remains at a low level. It becomes impossible for both prey and predator to coexist if the fear effect or prey harvesting exerts a pronounced impact. As the fear effect or constant-type harvesting become large, system (4) transitions from a stable state to an unstable state. These findings suggest that system (4) exhibits more intricate dynamic behaviors compared to the systems studied in previous works by [22] and [6].

Author contributions. The authors (C.H. and Z.L.) have contributed as follows: methodology, formal analysis, software, writing – original draft preparation, writing – review and editing, C.H.; formal analysis, validation, writing – review and editing, Z.L. All authors have read and approved the published version of the manuscript.

Conflicts of interest. The authors declare no conflicts of interest.

References

1. L.T. Bhutia, S. Biswas, E. Das, T.K. Kar, Evolution of Turing patterns of a predator–prey system with variable carrying capacity and harvesting, *Chaos Solitons Fractals*, **191**:115790, 2025, https://doi.org/10.1016/j.chaos.2024.115790.
2. S. Biswas, L.T. Bhutia, T.K. Kar, B. Bhutia, E. Das, Spatiotemporal analysis of a modified Leslie–Gower model with cross-diffusion and harvesting, *Physica D*, **470**:134381, 2024, https://doi.org/10.1016/j.physd.2024.134381.
3. M. Chen, Y. Takeuchi, J.-F. Zhang, Dynamic complexity of a modified Leslie–Gower predator–prey system with fear effect, *Commun. Nonlinear Sci. Numer. Simul.*, **119**:107109, 2023, https://doi.org/10.1016/j.cnsns.2023.107109.

4. Y. Dai, Y. Zhao, B. Sang, Four limit cycles in a predator–prey system of Leslie type with generalized Holling type III functional response, *J. Differ. Equations*, **50**:218–239, 2019, https://doi.org/10.1016/j.nonrwa.2019.04.003.

5. D. Das, T.K. Kar, D. Pal, The impact of invasive species on some ecological services in a harvested predator–prey system, *Math. Comput. Simul.*, **212**:66–90, 2023, https://doi.org/10.1016/j.matcom.2023.04.024.

6. Y.-J. Gong, J.-C. Huang, Bogdanov-Takens bifurcation in a Leslie-Gower predator-prey model with prey harvesting, *Acta Math. Appl. Sin., Engl. Ser.*, **30**:239–244, 2014, https://doi.org/10.1007/s10255-014-0279-x.

7. M. He, Z. Li, Global dynamics of a Leslie–Gower predator–prey model with square root response function, *Appl. Math. Lett.*, **140**:108561, 2023, https://doi.org/10.1016/j.aml.2022.108561.

8. D. Hu, H. Cao, Stability and bifurcation analysis in a predator–prey system with Michaelis–Menten type predator harvesting, *Nonlinear Anal., Real World Appl.*, **33**:58–82, 2017, https://doi.org/10.1016/j.nonrwa.2016.05.010.

9. J. Huang, Y. Gong, J. Chen, Multiple bifurcations in a predator–prey system of Holling and Leslie type with constant-yield prey harvesting, *Int. J. Bifurcation Chaos Appl. Sci. Eng.*, **23**:1350164, 2024, https://doi.org/10.1142/s0218127413501642.

10. P.H. Leslie, Some further notes on the use of matrices in population mathematics, *Biometrika*, **35**(3/4):213–245, 1948, https://doi.org/10.2307/2332342.

11. Y. Li, M. He, Z. Li, Dynamics of a ratio-dependent Leslie–Gower predator–prey model with Allee effect and fear effect, *Math. Comput. Simul.*, **201**:417–439, 2022, https://doi.org/10.1016/j.matcom.2022.05.017.

12. M. Lu, J. Huang, S. Ruan, P. Yu, Bifurcation analysis of an SIRS epidemic model with a generalized nonmonotone and saturated incidence rate, *J. Differ. Equations*, **267**:1859–1898, 2019, https://doi.org/10.1016/j.jde.2019.03.005.

13. L. Perko, *Differential Equations and Dynamical Systems*, Springer, New York, 2013, https://doi.org/10.1007/978-1-4684-0392-3.

14. S.K. Sasmal, Y. Takeuchi, Dynamics of a predator-prey system with fear and group defense, *J. Math. Anal. Appl.*, **481**:123471, 2020, https://doi.org/10.1016/j.jmaa.2019.123471.

15. J.-G. Wang, X.-Y. Meng, L. Lv, J. Li, Stability and bifurcation analysis of a Beddington–Deangelis prey–predator model with fear effect, prey refuge and harvesting, *Int. J. Bifurcation Chaos Appl. Sci. Eng.*, **33**:2350013, 2023, https://doi.org/10.1142/S021812742350013X.

16. X. Wang, L. Zanette, X. Zou, Modelling the fear effect in predator–prey interactions, *J. Math. Biol.*, **73**:1179–1204, 2016, https://doi.org/10.1007/s00285-016-0989-1.

17. H. Wu, Z. Li, M. He, Bifurcation analysis of a Holling–Tanner model with generalist predator and constant-yield harvesting, *Int. J. Bifurcation Chaos Appl. Sci. Eng.*, **34**:2450076, 2025, https://doi.org/10.1142/S0218127424500767.

18. C. Xiang, J. Huang, H. Wang, Bifurcations in Holling-Tanner model with generalist predator and prey refuge, *J. Differ. Equations*, **343**:495–529, 2023, https://doi.org/10.1016/j.jde.2022.10.018.

19. A. Yang, H. Wang, S. Yuan, Tipping time in a stochastic Leslie predator–prey model, *Chaos Solitons Fractals*, **171**:113439, 2023, https://doi.org/10.1016/j.chaos.2023.113439.

20. W. Yin, Z. Li, F. Chen, M. Xe, Modeling Allee effect in the Leslie-Gower predator–prey system incorporating a prey refuge, *Int. J. Bifurcation Chaos Appl. Sci. Eng.*, **32**:2250086, 2022, https://doi.org/10.1142/S0218127422500869.

21. Z.-F. Zhang, T.-R. Ding, W.-Z. Huang, Z.-X. Dong, *Qualitative Theory of Differential Equations*, Transl. Math. Monogr., Vol. 101, AMS, Providence, RI, 1992, https://doi.org/10.1090/mmono/101.

22. C.R. Zhu, K.Q. Lan, Phase portraits, Hopf bifurcations and limit cycles of Leslie-Gower predator-prey systems with harvesting rates, *Discrete Contin. Dyn. Syst., Ser. B*, **14**:289–306, 2010, https://doi.org/10.3934/dcdsb.2010.14.289.